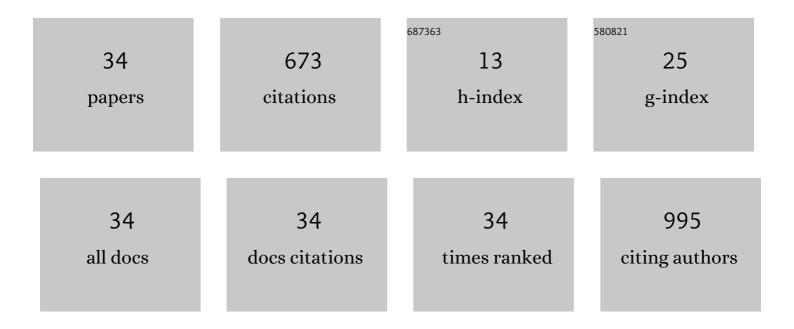
## Hui-Juan You

List of Publications by Year in descending order

Source: https://exaly.com/author-pdf/177859/publications.pdf Version: 2024-02-01



#	Article	IF	CITATIONS
1	Oxygen-Challenge Blood Oxygen Level-Dependent Magnetic Resonance Imaging for Evaluation of Early Change of Hepatocellular Carcinoma to Chemoembolization: A Feasibility Study. Academic Radiology, 2021, 28, S13-S19.	2.5	3
2	Noninvasive Differentiation of Obstructive Azoospermia and Nonobstructive Azoospermia Using Multimodel Diffusion Weighted Imaging. Academic Radiology, 2021, 28, 1375-1382.	2.5	2
3	Mechanical diversity and folding intermediates of parallel-stranded G-quadruplexes with a bulge. Nucleic Acids Research, 2021, 49, 7179-7188.	14.5	9
4	Characterization of G-Quadruplexes Folding/Unfolding Dynamics and Interactions with Proteins from Single-Molecule Force Spectroscopy. Biomolecules, 2021, 11, 1579.	4.0	17
5	Using Magnetic Tweezers to Unravel the Mechanism of the G-quadruplex Binding and Unwinding Activities of DHX36 Helicase. Methods in Molecular Biology, 2021, 2209, 175-191.	0.9	5
6	Single-Molecule Mechanical Unfolding of AT-Rich Chromosomal Fragile Site DNA Hairpins: Resolving the Thermodynamic and Kinetic Effects of a Single G-T Mismatch. Journal of Physical Chemistry B, 2020, 124, 9365-9370.	2.6	5
7	High Mechanical Stability and Slow Unfolding Rates Are Prevalent in Parallel-Stranded DNA G-Quadruplexes. Journal of Physical Chemistry Letters, 2020, 11, 7966-7971.	4.6	12
8	Discrimination between benign and malignant testicular lesions using volumetric apparent diffusion coefficient histogram analysis. European Journal of Radiology, 2020, 126, 108939.	2.6	13
9	Detecting the Formation Kinetics of Doxorubicin-DNA Interstrand Cross-link at the Single-Molecule Level and Clinically Relevant Concentrations of Doxorubicin. Analytical Chemistry, 2020, 92, 4504-4511.	6.5	9
10	Sight and switch off: Nerve density visualization for interventions targeting nerves in prostate cancer. Science Advances, 2020, 6, eaax6040.	10.3	28
11	A Universal Assay for Making DNA, RNA, and RNA–DNA Hybrid Configurations for Single-Molecule Manipulation in Two or Three Steps without Ligation. ACS Synthetic Biology, 2019, 8, 1663-1672.	3.8	10
12	Validation of SE-EPI-based T2 mapping for characterization of prostate cancer: a new method compared with the traditional CPMG method. Abdominal Radiology, 2019, 44, 3432-3440.	2.1	2
13	Bi-exponential versus mono-exponential diffusion-weighted imaging for evaluating prostate cancer aggressiveness after radical prostatectomy: a whole-tumor histogram analysis. Acta Radiologica, 2019, 60, 1566-1575.	1.1	4
14	Multi-parametric MRI-based radiomics signature for discriminating between clinically significant and insignificant prostate cancer: Cross-validation of a machine learning method. European Journal of Radiology, 2019, 115, 16-21.	2.6	95
15	Folding/unfolding kinetics of G-quadruplexes upstream of the P1 promoter of the human BCL-2 oncogene. Journal of Biological Chemistry, 2019, 294, 5890-5895.	3.4	43
16	T2-Weighted Image-Based Radiomics Signature for Discriminating Between Seminomas and Nonseminoma. Frontiers in Oncology, 2019, 9, 1330.	2.8	23
17	The Mechanical Properties of RNA-DNA Hybrid Duplex Stretched by Magnetic Tweezers. Biophysical Journal, 2019, 116, 196-204.	0.5	40
18	Effects of Echo Time on IVIM Quantification of the Normal Prostate. Scientific Reports, 2018, 8, 2572.	3.3	13

Hui-Juan You

#	Article	IF	CITATIONS
19	Two-State Folding Energy Determination Based on Transition Points in Nonequilibrium Single-Molecule Experiments. Journal of Physical Chemistry Letters, 2018, 9, 811-816.	4.6	11
20	Multi-model Analysis of Diffusion-weighted Imaging of Normal Testes at 3.0 T. Academic Radiology, 2018, 25, 445-452.	2.5	4
21	ZYH005, a novel DNA intercalator, overcomes all-trans retinoic acid resistance in acute promyelocytic leukemia. Nucleic Acids Research, 2018, 46, 3284-3297.	14.5	13
22	Characterization of testicular germ cell tumors: Whole-lesion histogram analysis of the apparent diffusion coefficient at 3T. European Journal of Radiology, 2018, 98, 25-31.	2.6	15
23	Single-molecule imaging and manipulation of biomolecular machines and systems. Biochimica Et Biophysica Acta - General Subjects, 2018, 1862, 241-252.	2.4	12
24	Diagnostic Performance and Interobserver Consistency of the Prostate Imaging Reporting and Data System Version 2. Chinese Medical Journal, 2018, 131, 1666-1673.	2.3	9
25	Structural–elastic determination of the force-dependent transition rate of biomolecules. Chemical Science, 2018, 9, 5871-5882.	7.4	45
26	Single-molecule Manipulation of G-quadruplexes by Magnetic Tweezers. Journal of Visualized Experiments, 2017, , .	0.3	4
27	RHAU helicase stabilizes G4 in its nucleotide-free state and destabilizes G4 upon ATP hydrolysis. Nucleic Acids Research, 2017, 45, 206-214.	14.5	40
28	Stability and Kinetics of c- <i>MYC</i> Promoter G-Quadruplexes Studied by Single-Molecule Manipulation. Journal of the American Chemical Society, 2015, 137, 2424-2427.	13.7	81
29	Torque Transmission Mechanism via DELSEED Loop of F1-ATPase. Biophysical Journal, 2015, 108, 1144-1152.	0.5	15
30	Dynamics and stability of polymorphic human telomeric G-quadruplex under tension. Nucleic Acids Research, 2014, 42, 8789-8795.	14.5	79
31	Winding DNA on Molecular Reel Made of F <sub>1</sub> -ATPase. Seibutsu Butsuri, 2013, 53, 160-161.	0.1	0
32	Winding single-molecule double-stranded DNA on a nanometer-sized reel. Nucleic Acids Research, 2012, 40, e151-e151.	14.5	12
33	3PT103 Bending stiffness of double-stranded DNA measured by winding single-molecule on a nanometer-sized reel(The 50th Annual Meeting of the Biophysical Society of Japan). Seibutsu Butsuri, 2012, 52, S157-S158.	0.1	0
34	1C1324 Flexural rigidity of dsDNA measured by winding single molecule on a nanometer size bearing(Nucleic acid,The 49th Annual Meeting of the Biophysical Society of Japan). Seibutsu Butsuri, 2011, 51, S34.	0.1	0